

# Polarized x-ray absorption spectra of $\text{CuGeO}_3$ at the Cu and Ge $K$ edges

O. Šipr and A. Šimůnek

*Institute of Physics, Academy of Sciences of the Czech Republic,  
Cukrovarnická 10, 162 53 Praha 6, Czech Republic*

S. Bocharov

*Hasylab at DESY, Notkestr. 85, D-22603 Hamburg, Germany*

G. Dräger

*Fachbereich Physik der Martin-Luther-Universität Halle-Wittenberg,  
Friedemann-Bach-Platz 6, D-06108 Halle, Germany,*

(August 14, 2002)

## Abstract

Polarized x-ray absorption near edge structure (XANES) spectra at both the Cu and the Ge  $K$ -edges of  $\text{CuGeO}_3$  are measured and calculated relying on the real-space multiple-scattering formalism within a one-electron approach. The polarization components are resolved not only in the unit cell coordinate system ( $\epsilon \parallel a$ ,  $\epsilon \parallel b$ ,  $\epsilon \parallel c$ ) but also in a local frame attached to the nearest neighborhood of the photoabsorbing Cu atom. In that way, features which resist a particular theoretical description can be identified. We have found that it is the out-of- $\text{CuO}_4$ -plane  $p_{z'}$  component which defies the one-electron calculation based on the muffin-tin potential. For the Ge  $K$  edge XANES, the agreement between the theory and the experiment appears to be better for those polarization components which probe more compact local surroundings than for those which probe regions with lower atomic density.

*Paper published in Phys. Rev. B **66**, 155119 (2002) and available on-line at  
<http://link.aps.org/abstract/PRB/v66/e155119>.*

78.70.Dm

## I. INTRODUCTION

The main incentive for studying  $\text{CuGeO}_3$  comes from the fact that it exhibits the spin-Peierls transition.<sup>1</sup> Apart from that, it is a member of the very interesting family of copper oxides, which displays a manifold of outstanding physical properties. X-ray absorption spectroscopy (XAS) is a convenient tool for investigating low-lying unoccupied electron states, due to its chemical and angular selectivity. This is especially important for compounds, where by exploring different absorption edges, XAS is able to provide a comprehensive picture of the local electronic structure of the material in question. Further details can be obtained by analyzing polarized (i.e., angular-dependent) spectra, as in that way features which would be obscured in unpolarized spectra can be observed. Also, comparison with polarized experimental x-ray absorption spectra poses a much more stringent test to the theory.<sup>2</sup>

$\text{CuGeO}_3$  has an orthorhombic crystal structure<sup>3</sup> with  $a=4.80$  Å,  $b=8.48$  Å, and  $c=2.94$  Å (space group no. 51, labeled  $Pbmm$  or  $D_{2h}^5$ ), therefore, its polarized spectra generated by dipole transitions can be decomposed into three partial spectral components.<sup>4</sup> While all Cu and all Ge atoms are equivalent within the symmetry properties of the lattice, there are two distinct O sites in the  $\text{CuGeO}_3$  crystal. Instructive pictures of the  $\text{CuGeO}_3$  structure can be found in Fig. 1 of Ref. 5, Fig. 1 of Ref. 6 or, from a more local point of view, in Fig. 1 of Ref. 7.

In the past, x-ray absorption near-edge structure (XANES) of the  $\epsilon||b$  and  $\epsilon||c$  polarized components at the Cu  $K$  edge was measured by Cruz *et al.*<sup>8</sup> and polarized O  $K$  edge spectra were measured by Corradini *et al.*<sup>9</sup> No measurement of the Ge  $K$  edge XANES has been reported so far. Cruz *et al.*<sup>8</sup> perform a theoretical analysis of the pre-peak relying on their many-body cluster calculation, Corradini *et al.*<sup>9</sup> compare the lowest in energy part of their spectra with densities of states around oxygen atoms as provided by many-body calculations of Villaflorita *et al.*<sup>10</sup> No attempts to calculate the spectra in the whole XANES range were made in either Ref. 8 or Ref. 9. Relying on quantitative arguments and on analogies with spectra of other compounds, Cruz *et al.*<sup>8</sup> suggest a many-body interpretation of the main Cu  $K$  edge XANES peak splitting.

Due to the presence of strong electron correlations in  $\text{CuGeO}_3$ , a one-particle approach apparently cannot be fully trusted for describing the states at the bottom of the conduction band (pre-edge region, photoelectron energy  $E \lesssim 5$  eV above the threshold). It may be worthwhile, however, to apply the one-particle formalism based on the local density approximation (LDA) to the rest of the XANES region. One would be then able to complement qualitative and empirical arguments, which have been applied for interpreting  $\text{CuGeO}_3$  spectra in this energy domain so far, with a material-specific *ab-initio* approach.

In our study, we investigate polarized XANES spectra at the Cu  $K$  edge and the Ge  $K$  edge, both experimentally and theoretically. By recording the spectra for several orientations of the crystal with respect to the x-ray polarization vector  $\epsilon$ , we are able to explore not only the  $\epsilon||b$  and  $\epsilon||c$  polarizations analyzed by Cruz *et al.*<sup>8</sup> but also the remaining  $\epsilon||a$  component. Our theoretical treatment is based on the multiple-scattering formalism in the real space. For a more comprehensive insight into the physical nature of the electron states probed by the Cu  $K$  edge XANES, we resolve the polarization components not only in the unit cell coordinate system but also in a local reference frame attached to the coordination polyhedron

of the photoabsorbing Cu atom. In that way, features which defy a particular theoretical description can be specifically identified. As we include also the Ge edge into our study, a complete view of the structure of unoccupied electron states in  $\text{CuGeO}_3$  as seen from the copper, germanium, and oxygen<sup>9</sup> sites emerges finally.

## II. RESULTS

### A. Experiment

We used an experimental setup very similar to that described in a greater detail in our previous publications.<sup>2,11</sup> The layered structure of  $\text{CuGeO}_3$  allows to prepare a sample for x-ray transmission experiments through splitting a single-crystal slab into thin plates perpendicular to the unit cell direction  $a$ . A plate of about  $7\text{ mm} \times 4\text{ mm} \times 0.03\text{ mm}$  was separated from the slab by means of usual scalpel and immediately used as the sample. The experiments were carried out at the beam lines A1 and E4 (HASYLAB, DESY) equipped with an Si (111) two crystal monochromator. For detection of the x-ray intensities in front of and behind the sample plate, usual ionization chambers were used. The sample plate was positioned in a PC-controlled goniometer, allowing three perpendicular rotations. In that way, several polarized spectra for various orientations of the polarization vector  $\epsilon$  with respect to the sample were recorded. In order to separate the absorption resulting from the  $K$ -transitions exclusively, we used a subtraction of the background function  $f(E) = a/E^4 + b/E^3 + c$  after Victoreen. All the spectra were corrected for an equivalent effective sample thickness, with an additional matching normalization of  $\max \pm 5\%$  in the remote extended x-ray absorption fine structure (EXAFS) region. Some of the measured curves are displayed in Fig. 1 (Cu edge) and Fig. 2 (Ge edge) for several representative orientations of the polarization vector  $\epsilon$  with respect to the  $\text{CuGeO}_3$  monocystal.

### B. Symmetry decomposition

Theoretical foundations needed for extracting symmetry-resolved partial spectral components of x-ray absorption spectra were outlined by Brouder<sup>4</sup> in an extensive way. For an orthorhombic crystal, in particular, any polarized x-ray absorption spectrum can be decomposed into a weighted sum of three independent partial spectral components (in the dipole approximation). These partial spectral components can be chosen so that they correspond to the polarized spectra recorded with the  $\epsilon$  vectors parallel to each of the crystal axes. Hence, the dipole part of any linearly polarized spectrum can be written as<sup>2,11</sup>

$$\mu_D = p_x \epsilon_x^2 + p_y \epsilon_y^2 + p_z \epsilon_z^2 \quad , \quad (1)$$

where  $\epsilon_x$ ,  $\epsilon_y$ , and  $\epsilon_z$  are cartesian components of the polarization vector  $\epsilon$  and  $p_x$ ,  $p_y$ , and  $p_z$  denote the partial spectral components (their designation reflects the corresponding projected density of states). Note that our Eq. (1) can be transformed into the tensor form presented by Brouder<sup>4</sup> by simple algebraic manipulations.

By inverting Eq. (1) for a triad of measured spectra, the partial spectral components in a unit cell reference frame can be extracted (i.e., we take  $x||a$ ,  $y||b$ , and  $z||c$  — see Fig. 3

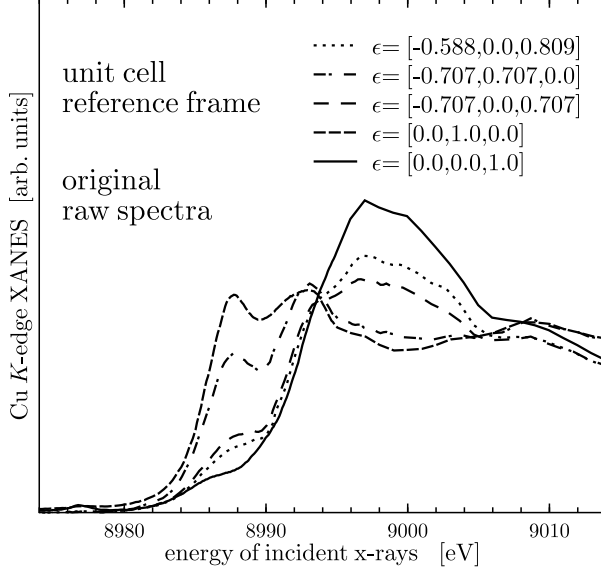


FIG. 1. Measured XANES curves at the Cu edge of  $\text{CuGeO}_3$  for several representative orientations of the polarization vector  $\epsilon$  with respect to the  $\text{CuGeO}_3$  monocrystal. The projected components of the  $\epsilon$  vector on the crystal unit cell axes  $a$ ,  $b$  and  $c$  are written in square parentheses in the legend.

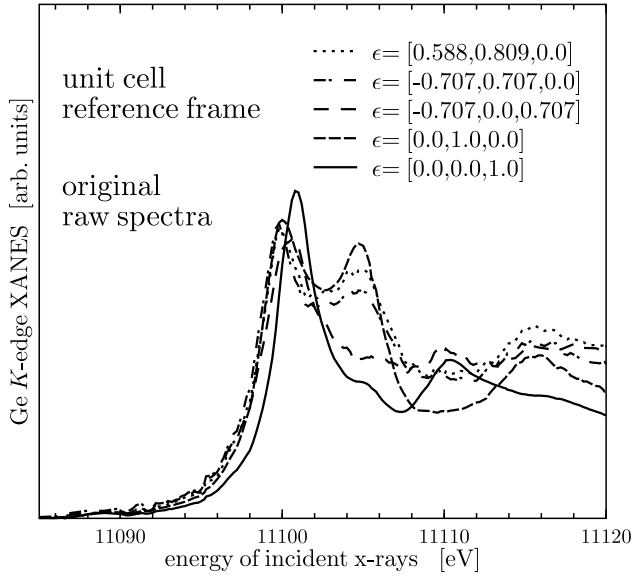


FIG. 2. Measured XANES curves at the Ge edge of  $\text{CuGeO}_3$  for several representative polarization vectors. This drawing is analogous to Fig. 1.

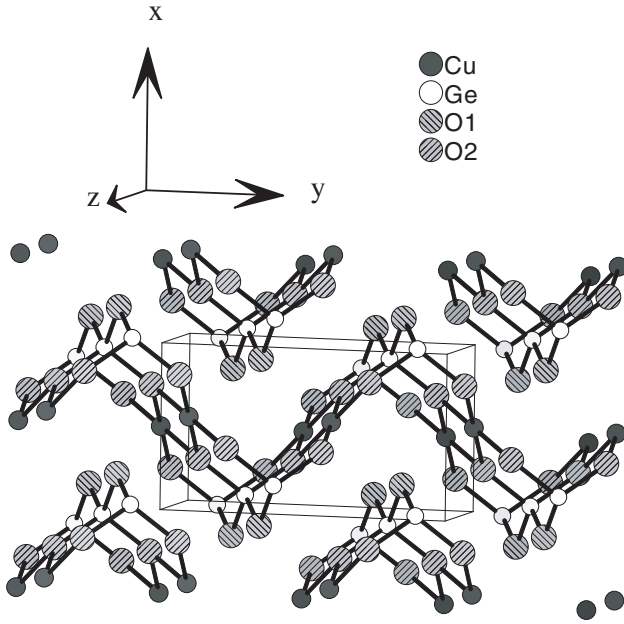


FIG. 3. A schematic depiction of the unit cell reference frame we use for decomposing the polarized spectra. The unit cell is drawn in the center of the plot. Atoms belonging to eight  $\text{CuGeO}_3$  unit cells are shown in total. The symbols O1 and O2 used in the legend refer to two inequivalent oxygen sites. Note that in this reference frame one has  $x \parallel a$ ,  $y \parallel b$ , and  $z \parallel c$ , as indicated.

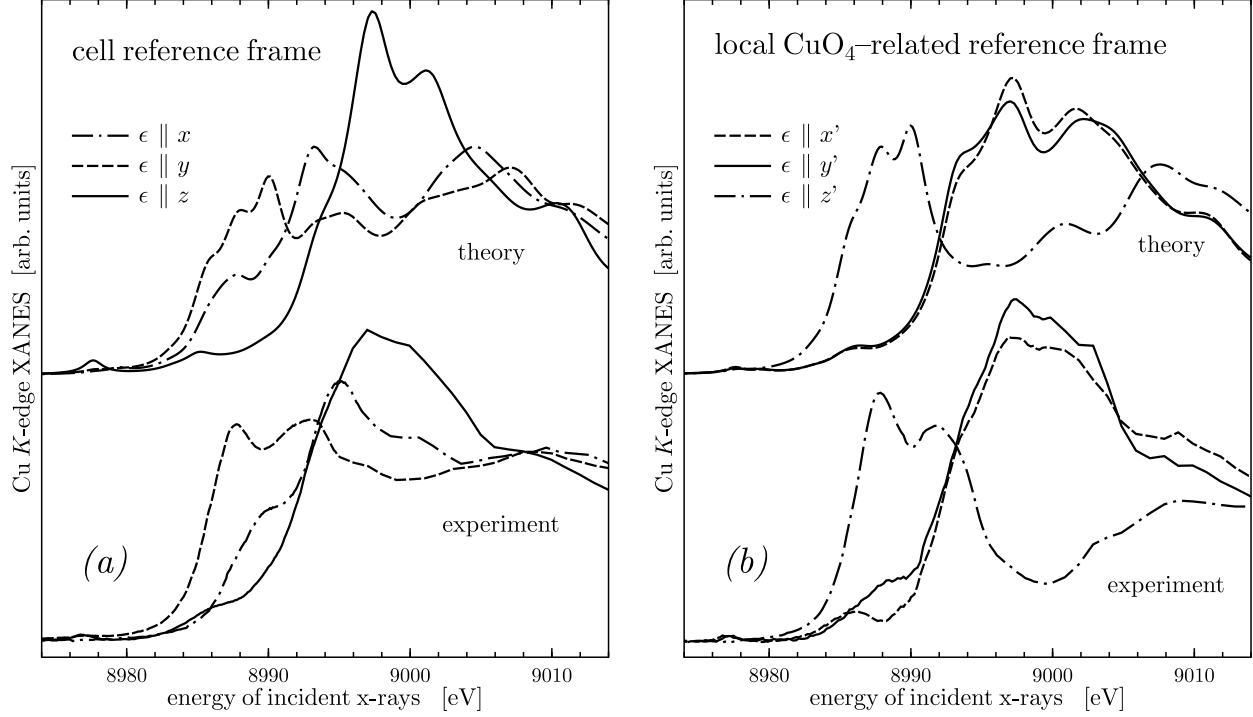


FIG. 4. (a) Experimental (lower graph) and theoretical (upper graph) Cu  $K$  edge polarized XANES partial spectral components  $p_x$ ,  $p_y$ , and  $p_z$  resolved in a unit cell reference frame. (b) Experimental (lower graph) and theoretical (upper graph) Cu  $K$  edge partial spectral components  $p_{x'}$ ,  $p_{y'}$ , and  $p_{z'}$  resolved in a local reference frame attached to the nearest Cu neighborhood. The theoretical curves were obtained for a cluster of 167 atoms, taking into account a relaxed and screened core hole.

for a schematic depiction). The results of such a decomposition of experimental spectra are shown in the lower graphs of Fig. 4a for the Cu  $K$  edge and of Fig. 5 for the Ge  $K$  edge. We checked that the partial spectral components obtained in this way do not depend on the particular choice of the triad of experimental spectra which was involved in inversion of Eq. (1) (see also Refs. 2, 11 for a more thorough discussion). Our  $p_y$  and  $p_z$  components of the Cu  $K$  edge XANES are in a good agreement with the corresponding  $\epsilon||b$  and  $\epsilon||c$  components measured by Cruz *et al.*<sup>8</sup> The remaining  $p_x$  component cannot be measured directly for a crystal cleaved parallel to the  $bc$  plane and is best accessible through the kind of decomposition we performed here.

By considering the quadrupole transitions as well, one might be able to separate the dipole and the quadrupole contributions in the pre-peaks at 8977 eV and at 11089 eV and even to estimate the angular character of the quadrupole parts, analogously as it was done for CuO.<sup>11</sup> However, the pre-peak intensity is too low in this case to allow a reliable analysis of this kind. Therefore, we limit ourselves to exploring dipole transitions exclusively.

In order to get a better physical insight into the nature of the some spectral features, one may attempt to perform the spectral decomposition in other coordinate frames as well. In particular, this might be especially useful in a reference frame which reflects the *local* symmetry around the photoabsorbing site. Although Eq. (1) is strictly valid in the unit

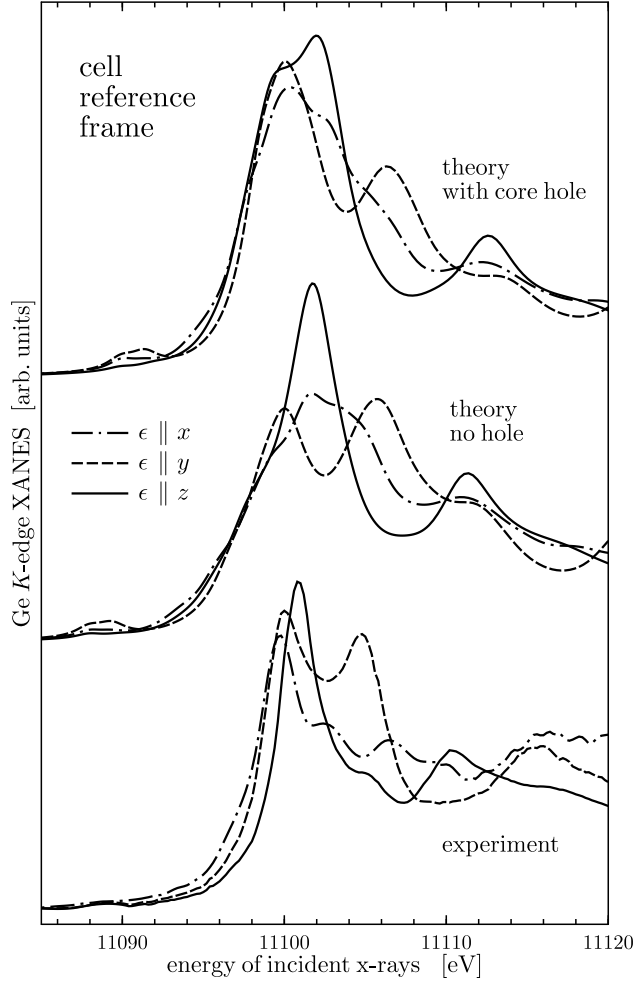


FIG. 5. Experimental (lower graph) and theoretical (two upper graphs) Ge  $K$  edge XANES partial spectral components  $p_x$ ,  $p_y$ , and  $p_z$  resolved in a unit cell reference frame. Theoretical curves obtained for a cluster of 169 atoms are shown both for a ground state potential (no core hole) as well as for the case when a relaxed and screened core hole is taken into account.

cell reference frame only, it has been demonstrated that a consistent resolving of partial spectral components may be possible in local reference frames as well, provided that the coordinate axes are chosen in a suitable way.<sup>11</sup> One can make an *a posteriori* check whether the coordinate frame was chosen in a suitable way or not by performing the inversion of Eq. (1) for several independent triads of measured spectra. Only if the partial spectral components obtained from different sets of data coincide, the corresponding coordinate system is a “good” one. The physical interpretation of partial components in such a local-symmetry-adapted system is often more transparent than in the case of a unit cell reference frame and may be more suitable for comparing spectra at absorption edges of atoms of the same element in different compounds.

The nearest neighborhood of Cu in CuGeO<sub>3</sub> is similar to that of other copper oxides: Copper is in the center of an oxygen rectangle. Four nearest oxygens at a distance of 1.93 Å form its corners, the sides of the rectangle are 2.50 Å and 2.94 Å long, respectively. As can be seen from Fig. 3, there are actually two interpenetrating networks of CuO<sub>4</sub> rectangles in a CuGeO<sub>3</sub> crystal, tilted one to another at an angle of 69°. Thus one has to take into account when inverting Eq. (1) that the measured spectra reflect in fact an average over Cu sites belonging to two different systems. A similar situation arises, e.g., in a pure copper oxide CuO (Ref. 11). We have found that the local partial spectral components  $p_{x'}$ ,  $p_{y'}$ , and  $p_{z'}$  at the Cu *K* edge XANES can be consistently resolved in a local reference frame where the  $z'$  axis is perpendicular to the CuO<sub>4</sub> plane, the  $x'$  axis coincides with a Cu-O bond and the  $y'$  axis is perpendicular to both  $x'$  and  $z'$  axes, meaning that it lies in the CuO<sub>4</sub> plane and holds a 9° angle with another Cu-O bond. A schematic drawing of the orientation of this local reference frame with respect to the CuO<sub>4</sub> rectangle is shown in Fig. 6. Partial spectral components resolved in the local reference frame are displayed in Fig. 4b. It should be noted that a consistent decomposition of Cu *K* edge XANES in CuGeO<sub>3</sub> cannot be obtained if one chooses the local  $x'$  and  $y'$  axes parallel to the sides of the CuO<sub>4</sub> rectangle (the partial components derived from different sets of measured spectra do not coincide in that case). Hence, the situation is just opposite to the case of CuO, where the partial components could be consistently resolved in a local reference frame only if the  $x'$ ,  $y'$  axes were parallel to the sides of the CuO<sub>4</sub> parallelogram.<sup>11</sup>

We did not attempt to decompose the Ge spectra in a local reference frame as our primary concern is the Cu edge in relation to spectra of other copper oxides.

### C. Theory

Theoretical Cu *K* edge and Ge *K* edge partial spectral components were evaluated by calculating XANES spectra with the polarization vector  $\epsilon$  being pointed to relevant directions. Self-consistent scattering potentials were taken over from SCF- $X\alpha$  molecular calculations<sup>12</sup> for clusters of 15–24 atoms, employing an amended XASCF code of Case and Cook.<sup>13,14</sup> The results presented in upper graphs of Figs. 4–5 were calculated using the real-space multiple-scattering (RS-MS) formalism,<sup>15</sup> employing clusters of 167 and 169 atoms for the Cu and Ge edges, respectively. These calculations were done using the RSMS code, which is an amended descendant of the ICXANES code<sup>16</sup> and is maintained by our group.<sup>17</sup> A few more technical details about our implementation of the RS-MS technique can be found elsewhere.<sup>11,18</sup> In order to verify the robustness of our results, we compared the results



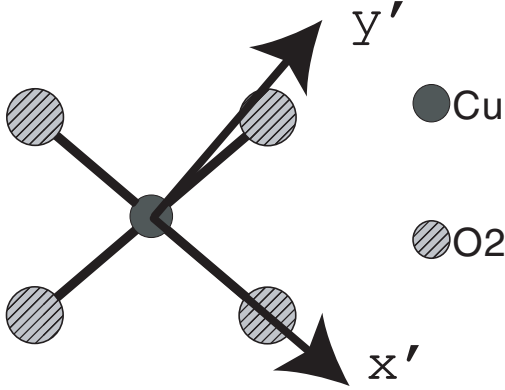


FIG. 6. The local reference frame used for resolving partial spectral components  $p_{x'}$ ,  $p_{y'}$ , and  $p_{z'}$  in this paper. The  $x'$  and  $y'$  axes are perpendicular to each other, the  $z'$  axis is perpendicular to the plane of the  $\text{CuO}_4$  rectangle.

obtained by our codes and by the selfconsistent FEFF8 code<sup>19</sup> (version 8.10). Both code packages rely on a bit different implementations of the one-electron multiple-scattering formalism: E.g., the interstitial region is suppressed in the stage of finding the selfconsistent potential in the FEFF8 code while we use a proper muffin-tin formalism and Norman muffin-tin sphere radii are employed in FEFF8 while we use matching-potential radii. Despite these differences, both codes gave similar results for identical clusters (we used 95 atoms for Cu edge and 91 atoms for Ge edge spectra in this comparative study). The main difference consisted in up to 20% lower intensities of some low-energy ( $E \lesssim 25$  eV) spectral peaks for the FEFF8 code, giving thus worse agreement with experiment than our XASCF and RSMS codes. We did not try to optimize FEFF8 input parameters to identify the source of this difference, our goal has been just to check that the two codes do not lead to contradictory pictures. A comparison of XANES spectra calculated for various settings of the muffin-tin potential parameters can be found, e.g., in Ref. 2.

The XANES calculations for 167/169-atoms clusters were performed both without any core hole and with a relaxed and screened core hole taken into account (i.e., a  $1s$  electron was removed from the central atom and put among the valence electrons and only thereafter the electronic structure of the cluster was selfconsistently calculated). Neither choice leads to essentially better agreement between the theory and experiment than the other one. Generally, the core hole increases the intensity of peaks at the low-energy part of the spectra. This effect is not significant at the Cu edge so we display only the results of the calculation which takes the core hole into consideration in Fig. 4 (the intensities of theoretical peaks at 8993 eV for the  $p_y$  component and at 8997 eV for the  $p_z$  component would be about 10% lower if the core hole was neglected). At the Ge edge the core hole effect is more significant so we display both sets of curves in Fig. 5. It appears that including the core hole actually “overcorrects” the ground state results in this case and consequently does not give rise to distinctly better agreement between theory and experiment for the Ge edge XANES.

We made analogous calculations for non-selfconsistent potentials constructed according to the Mattheiss prescription (superposition of potentials and charge densities of isolated atoms), too. As could be anticipated, selfconsistent potentials give rise to theoretical spectra

which agree better with experiment than in the case of non-selfconsistent potentials, however, the improvement is not an essential one. All distinct spectral features that can be observed at the theoretical curves in Figs. 4–5 are present also in corresponding spectra obtained for non-selfconsistent potentials, with peak positions and intensities differing no more than  $\approx 20\%$  (we do not show those curves for brevity). Thus use of self-consistent potentials is not crucial for our study.

The alignment in energy of the theoretical curves shown in Figs. 4–5 was set so that the best overall agreement between theory and experiment is achieved. All theoretical curves were convoluted with a Lorentzian function of the width  $w$  given by the *ansatz*  $w = w_c + 0.03 \times E$ , where the constant part  $w_c$  accounts for the core hole lifetime<sup>20</sup> and the energy-dependent part mimics the finite lifetime of a photoelectron with an energy  $E$ . The factor 0.03 was chosen just by convenience — we did not attempt to achieve the best possible agreement between theory and experiment by optimizing the smearing function.

### III. DISCUSSION

Let us concentrate first on the Cu  $K$  edge in the unit cell reference frame, where a partial comparison with the work of Cruz *et al.*<sup>8</sup> is possible. As it can be seen from Fig. 4a, our calculation describes the gross shape of the three components  $p_x$ ,  $p_y$ ,  $p_z$  and their polarization splitting. However, only the  $p_z$  component, probing states parallel to the  $c$  axis, is reproduced by the theory as concerns the number of features (shoulders at 8986 eV and 8993 eV and peaks at 8997 eV, 9000 eV, and 9008 eV at the experimental curve), their positions (within 1–2 eV's), and relative intensities. The reason why the two peaks of the main doublet in  $p_z$  are not clearly separated in the experiment (either ours or that of Cruz *et al.*<sup>8</sup>) is not clear. It may be a consequence of experimental energy resolution (most probably arising from the so called thickness effect — absorption maxima are suppressed and consequently smeared for thick samples) or it may stem from a smearing caused by many-body effects, not accounted for by our theory. The other two experimental components  $p_x$ ,  $p_y$  seem to include an ingredient which defies our theoretical description substantially more than is the case of the  $p_z$  component.

Cruz *et al.*<sup>8</sup> interpret the Cu  $K$  edge XANES of CuGeO<sub>3</sub> in this energy range by semi-quantitative arguments, relying on comparison with Cu spectra of La<sub>2</sub>CuO<sub>4</sub> and CuO. They suggest an essentially many-body interpretation of dominant spectral features: The double structure of the main peaks at 8987 eV and 8993 eV for the  $p_y$  component and at 8997 eV and 9000 eV for the  $p_z$  component (see Fig. 4a) is ascribed to transitions to well-screened final states followed by satellite transitions to poorly screened states. The success of our one-electron LDA-type computation to describe at least the  $p_z$  component correctly seems to contradict this point of view. Of course, no definite conclusion regarding the one-electron or many-body nature of the main  $p_z$  peak splitting can be made until a proper many-body calculation is done.

As noted above, the experimental  $p_x$  and  $p_y$  components in Fig. 4a display more serious deviations from the one-electron theory than the  $p_z$  component. In order to identify the source of these deviations, it might be useful to explore the partial spectral components in the local reference frame. Indeed, if we compare the theoretical and experimental curves in Fig. 4b, it emerges clearly that the primary source of discrepancy between the theory and the

experiment lies mainly *outside the CuO<sub>4</sub> plane*. The peak positions and relative intensities of the  $p_{x'}$  and  $p_{y'}$  components are reproduced by theory with a similar accuracy as was the case with the  $p_z$  component in the cell reference frame. The absence in the experiment of a well-defined doublet structure of the main peak at 8997–9004 eV is probably caused by the same mechanism as a similar situation with the cell  $p_z$  component mentioned above. The local  $p_{z'}$  component is described by the theory significantly worse than the local  $p_{x'}$  and  $p_{y'}$  components, especially as concerns the fine structure of the peak at 8988–8992 eV in Fig. 4b.

Having this in mind, one can re-assess the situation in the unit cell reference frame: As the  $c$  axis runs parallel to the CuO<sub>4</sub> plane, the  $p_z$  component probes solely states lying within this plane and, hence, can be correctly characterized by the theory (cf. Fig. 3). On the contrary, the  $p_x$  and  $p_y$  components probe states lying within the CuO<sub>4</sub> plane as well as states reaching perpendicular to it. It is the perpendicular-to-CuO<sub>4</sub> admixture into these components which spoils the agreement between theory and experiment. Without this mixing, one could have expected for Fig. 4a a similar agreement between the theory and experiment as can be seen in Fig. 4b for the  $p_{x'}$  and  $p_{y'}$  components.

The failure of the theory to describe the  $p_{z'}$  component in the local reference frame is not a total one: The theory accounts for the general trends of the  $p_{z'}$  spectral curve such as existence of a well-separated maximum at 8988–8992 eV followed by a broad structure around 9008 eV. The most notable deficiency of the theory for this polarization is not reproducing the double-peak structure at 8988 eV and 8992 eV. This failure then transforms into deficiencies in describing the unit cell  $p_x$  and  $p_y$  components in this energy region. Secondly, the fine structure of the second broad feature (positions and relative intensities of sub-maxima at 9003 eV and 9008 eV) is not correctly reproduced by our calculation.

At this point, it is difficult to identify the reason of this deficiency of the theory more specifically. One could make use of the analogy with La<sub>2</sub>CuO<sub>4</sub>, where the theory also describes the states within the Cu-O layers fairly accurately but fails in describing XANES components perpendicular to that layer.<sup>21,22</sup> Guo *et al*<sup>21</sup> attribute this failure to the presence of shake-up satellite peaks in La<sub>2</sub>CuO<sub>4</sub> spectra and present plausible arguments for their view. However, the situation may be different for CuGeO<sub>3</sub>: Among others, the failure of the theory for the out-of-plane XANES components appears to be much more dramatic for La<sub>2</sub>CuO<sub>4</sub> than for CuGeO<sub>3</sub> (a whole peak missing in La<sub>2</sub>CuO<sub>4</sub> spectrum vers. an inverted double-peak intensity in CuGeO<sub>3</sub> spectrum). Since the calculations of La<sub>2</sub>CuO<sub>4</sub> spectra<sup>21,22</sup> as well as our RS-MS calculation of CuGeO<sub>3</sub> XANES rely on the muffin-tin approximation, one cannot rule out full-potential effects as the main culprits. Intuitively one would expect non-muffin-tin corrections to be more important for the more loose out-of-plane states than for the states in the more closely-packed plane of CuO<sub>4</sub> rectangles, so this explanation would be in accord with our results. Anyway this question seems to remain open.

As can be seen from Fig. 4, the pre-peak at the Cu  $K$  edge appears to be reproduced at the correct position even if quadrupole transitions are neglected in the calculation. We verified that if the quadrupole transitions are included, they are completely negligible in the whole energy range except for the pre-edge region around 8977 eV, where they contribute with approximately with the same intensity as the dipole transitions. This might serve as an indication of a mixed dipole-quadrupole nature of the pre-peak at the Cu  $K$  edge of CuGeO<sub>3</sub>, however, one should be quite cautious about this issue as the successful reproduction of the

pre-peak position by our calculation may be just a fortuitous coincidence: The pre-edge XANES intensity crucially depends on the energy position of the onset of unoccupied states and on the structure of electronic states very close to this onset. This kind of information cannot be reliably obtained via an LDA-type calculation for a strongly-correlated material such as  $\text{CuGeO}_3$  (see Refs. 23, 24 for LDA calculations of electronic structure of  $\text{CuGeO}_3$  and Refs. 6, 7 for calculations going beyond LDA). Note that, e.g., in the case of  $\text{CuO}$  the agreement between theory and experiment in the pre-edge region is seemingly better for a non-selfconsistent potential than for a self-consistent one.<sup>18</sup> So we think that we cannot draw really reliable conclusions regarding the pre-edge region and, consequently, do not even display the corresponding “quadrupole-included” curves here.

The Ge  $K$  edge is decomposed in the unit cell reference frame in Fig. 5. As noted already in Sec. II C, the best agreement between theory and experiment would be attained for curves lying somewhat between the data obtained when the core hole is present and when it is neglected. Both calculations account for the strong polarization (i.e., angular) dependence of the experimental curves fairly well. However, not all components are described by the theory with the same accuracy. The main peak of the  $p_x$  component is too broad in the calculated spectra and neither the fine oscillations seen in the experimental  $p_x$  curve are reproduced by the theory appropriately (though including the core hole improves this a bit). The main doublet in the  $p_y$  component is reproduced, however, the separation of its peaks is 5 eV in the experiment and 6 eV in the theory. At the  $p_z$  component, the calculation without the core hole reproduces the 11101 eV and 11110 eV experimental peaks both in positions and relative intensities, just the 11105 eV shoulder is missing in the calculated curve. If the core hole is included, the low-energy shoulder at 11099 eV of the theoretical  $p_z$  curve is drastically increased, worsening thus the agreement with experiment. It seems therefore that a proper description of the core hole effect at the Ge edge of  $\text{CuGeO}_3$  has to go beyond the static relaxed and screened model. We did not try to employ other simple — less frequently used — prescriptions for core hole treatment (unrelaxed and/or unscreened hole) as they have not worked well with other non-metallic systems.<sup>25</sup>

Overall it appears that the best agreement between theory and experiment has been achieved for the  $\epsilon||c$  component  $p_z$ , next comes the  $\epsilon||b$  curve and, finally, worst agreement occurs for the  $\epsilon||a$  component  $p_x$ . Although we are unable to find unambiguously what is the reason for this “hierarchical” behavior, we believe that the degree of packing of the neighborhood of Ge atoms in various directions may be a factor. Namely, the Ge atoms are nearly tetrahedrally coordinated by four O atoms at 1.74–1.79 Å and the  $a$ ,  $b$ , and  $c$  directions hold different angles with those oxygens. The  $a$  direction avoids the tetrahedron corners as much as possible, holding a  $54^\circ$  angle with all the Ge-O bonds. The minimum angle between the  $b$  and  $c$  directions and any of the Ge-O bonds is  $36^\circ$ , on the other hand. Moreover, the  $c$  direction points exactly to the Ge atoms which form the second coordination shell around germanium at 2.94 Å. Hence, a rule of thumb emerges that the more open is the local geometry probed by a particular spectral component  $p_x$ ,  $p_y$ , or  $p_z$ , the worse agreement between theory and experiment at the Ge  $K$  edge arises. A possible explanation of this correlation might rest with the muffin-tin approximation we employ, as non muffin-tin effects are expected to be more significant at open geometries than at close ones.

Experimental XANES spectra at the O  $K$  edge of  $\text{CuGeO}_3$  were presented by Corradini *et al*<sup>9</sup> and by Agui *et al*<sup>26</sup> for energies up to 25 eV above the absorption threshold. The

interpretation of O edge spectra is complicated by the fact that there are two inequivalent oxygen sites in  $\text{CuGeO}_3$ , meaning that one sees a superposition of two edges in the experiment actually. We attempted to reproduce the polarization dependence of the O  $K$  edge spectra measured by Corradini *et al*<sup>9</sup> by a RS-MS calculation for the same self-consistent potential which we employed for calculating the curves displayed in Figs. 4–5. The energy shift between the edges of the two inequivalent oxygens was set by hand, as there are several factors affecting its value which cannot be described with a sufficient accuracy by an LDA-type calculation (a brief discussion of those effects can be found, e.g., in Ref. 9). We have found that there is no suitable value of such a shift which would lead to the reproduction of the two distinct polarization-dependent peaks within the first 3 eV above the O  $K$  edge threshold, as observed in the experiment.<sup>9</sup> On the other hand, the relatively broad main peak at 5–10 eV above the threshold does not exhibit any distinct angular-dependent features at all and, consequently, can be at least roughly reproduced for several different values of the energy shift between the two O edges, offering thus no clue for its proper value. We do not display the results here for brevity, concluding that our calculation cannot be used as a guide for interpreting the polarization dependence of the O  $K$  edge absorption spectrum of  $\text{CuGeO}_3$ . Strong electron correlations, unaccounted for by the LDA framework, seem to be the most probable explanation for the failure of our calculations to reproduce the polarized O  $K$  edge XANES close to the threshold. Note that for that reason (unreliability of LDA at the x-ray absorption threshold in  $\text{CuGeO}_3$ ) we do not discuss the pre-peaks at the Cu and Ge edges in detail either. On the other hand, those parts of the spectra which correspond to photoelectron energies higher than  $E \gtrsim 5$  eV can be at least partially described by a one-electron LDA-type approach, as demonstrated above (Figs. 4–5).

The fact that a relatively simple theory appears to be able to reproduce gross trends in XANES of an insulating, probably charge-transfer oxide is quite surprising on its own. It seems that strong electron correlations in this type of compound need not be so crucial at photoelectron energies *above the pre-edge*, contrary to what has been generally anticipated so far.

#### IV. CONCLUSIONS

The main features of polarized Cu  $K$  edge and Ge  $K$  edge XANES of  $\text{CuGeO}_3$  can be described fairly well within the one-electron framework. Contrary to earlier suggestions,<sup>8</sup> the main peak splitting for the  $\epsilon||c$  polarization at the Cu  $K$  edge can be correctly reproduced within the one-electron LDA-type approach (no need for superpositioning of well-screened and poorly-screened states). The source of the remaining discrepancies between theory and experiment at the Cu  $K$  edge XANES can be better identified and understood if the polarized spectra are decomposed in the local reference frame attached to the nearest Cu neighborhood rather than in the unit cell reference frame. We have found that it is the out-of- $\text{CuO}_4$ -plane  $p_z$  component which defies the one-electron RS-MS calculation for a muffin-tin potential. For the Ge  $K$  edge XANES, the agreement between the theory and the experiment appears to be better for those polarization components which probe more compact local surroundings than for those which are directed to the interstitial parts of the crystal. Including the core hole affects the Ge edge theoretical spectra significantly more than at the Cu edge and, to a certain degree, leads to a worse agreement with Ge edge experiment in comparison with

the case when the core hole is neglected.

### **ACKNOWLEDGEMENTS**

The theoretical part of this work was supported by grant 202/02/0841 of the Grant Agency of the Czech Republic. The experimental part was supported by Hamburger Synchrotronstrahlungslabor HASYLAB Project No. II-98-058. The use of the CRYSTIN structural database<sup>27</sup> was financed by grant 203/02/0436 of the Grant Agency of the Czech Republic.

## REFERENCES

- <sup>1</sup> M. Hase, I. Terasaki, and K. Uchinokura, Phys. Rev. Lett. **70**, 3651 (1993).
- <sup>2</sup> O. Šipr, A. Šimůnek, S. Bocharov, Th. Kirchner, and G. Dräger, Phys. Rev. B **60**, 14115 (1999).
- <sup>3</sup> S. Bräuning, U. Schwarz, M. Hanfland, T. Zhou, R. K. Kremer, and K. Syassen, Phys. Rev. B **56**, R11357 (1997).
- <sup>4</sup> C. Brouder, J. Phys.: Condens. Matter **2**, 701 (1990).
- <sup>5</sup> F. Parmigiani, L. Sangaletti, A. Goldoni, U. del Pennino, C. Kim, Z.-X. Shen, A. Revcolevschi, and G. Dhalenne, Phys. Rev. B **55**, 1459 (1997).
- <sup>6</sup> S. Atzkern, M. Knapfer, M. S. Golden, J. Fink, A. Hübsch, C. Waidacher, K. W. Becker, W. von der Linden, M. Weiden, and C. Geibel, Phys. Rev. B **64**, 075112 (2001).
- <sup>7</sup> S. Zagoulaev and I. I. Tupitsyn, Phys. Rev. B **55**, 13528 (1997).
- <sup>8</sup> D. Z. Cruz, M. Abbate, H. Tolentino, P. J. Schiling, E. Morikawa, A. Fujimori, and J. Akimitsu, Phys. Rev. B **59**, 12450 (1999).
- <sup>9</sup> V. Corradini, A. Goldoni, F. Parmigiani, C. Kim, A. Revcolevschi, L. Sangaletti, and U. del Pennino, Surf. Sci. **420**, 142 (1999).
- <sup>10</sup> A. Villaflorita, F. Manghi, F. Parmigiani, and C. Calandra, Solid State Commun. **104**, 301 (1997).
- <sup>11</sup> S. Bocharov, Th. Kirchner, G. Dräger, O. Šipr, and A. Šimůnek, Phys. Rev. B **63**, 045104 (2001).
- <sup>12</sup> K. H. Johnsson, Adv. Quantum Chem. **7** 143 (1973).
- <sup>13</sup> M. Cook and D. A. Case, computer code XASCF, Quantum Chemistry Program Exchange, Indiana University, Bloomington, Indiana (1980).
- <sup>14</sup> O. Šipr, F. Rocca, and G. Dalba, J. Synchrotron Rad. **6**, 770 (1999).
- <sup>15</sup> D. D. Vvedensky, in *Unoccupied Electronic States*, edited by J. C. Fuggle and J. E. Inglesfield (Berlin, Springer, 1992), p. 139.
- <sup>16</sup> D. D. Vvedensky, D. K. Saldin, J. B. Pendry, Comput. Phys. Commun. **40**, 421 (1986).
- <sup>17</sup> O. Šipr, computer code RSMS, Institute of Physics AS CR, Prague (1996-1999).
- <sup>18</sup> O. Šipr and A. Šimůnek, J. Phys.: Condens. Matter **13**, 8519 (2001).
- <sup>19</sup> A. L. Ankudinov, B. Ravel, J. J. Rehr, and S. D. Conradson, Phys. Rev. B **58**, 7565 (1998).
- <sup>20</sup> F. Al Shamma, M. Abbate, and J. C. Fuggle, in *Unoccupied Electron States*, edited by J. C. Fuggle and J. E. Inglesfield (Springer, Berlin, 1992), p. 347.
- <sup>21</sup> J. Guo, D. E. Ellis, G. L. Goodman, E. E. Alp, L. Soderholm, and G. K. Shenoy, Phys. Rev. B **41**, 82 (1990).
- <sup>22</sup> C. Li, M. Pompa, A. Congiu-Castellano, S. Della Longa, and A. Bianconi, Physica C **175**, 369 (1991).
- <sup>23</sup> L. F. Mattheiss, Phys. Rev. B **49**, 14050 (1994).
- <sup>24</sup> Z. S. Popović, F. R. Vukajlović, and Z. V. Šljivančanin, J. Phys.: Condens. Matter **7**, 4549 (1995).
- <sup>25</sup> O. Šipr, P. Machek, A. Šimůnek, J. Vackář, and J. Horák, Phys. Rev. B **56**, 13151 (1997).
- <sup>26</sup> A. Agui, J.-H. Guo, C. Sâthe, J. Nordgren, M. Hidaka, and I. Yamada, Solid State Commun. **118**, 619 (2001).
- <sup>27</sup> G. Bergerhoff, R. Hundt, R. Sievers, and I. D. Brown, J. Chem. Inform. Comput. Sci. **23**, 66 (1983).